ELECTRICAL CHARACTERIZATION OF NANOCRYSTALLINE ZINC OXIDE/ POURS SILICON HETEROJUNCTION FOR SOLAR CELLS

R. I. MOHAMMED, J. F. MOHAMMAD[*]
University of Anbar, College of education for pure Sciences, Physics Department, Iraq

Nanocrystalline Zinc Oxide (ZnO) were deposited at three different temperature (250, 300 and 350 ℃) using chemical spray pyrolysis technique (CSPT) on glass and p-type porous silicon as a substrates separately. The pours silicon was prepared by using an electrochemical etching process under a density of 40 mA/cm^2 for 10 minutes. Surface morphology results using atomic force microscopy (AFM) showed that the prepared films nanocrystalline structures, homogeneous surfaces with small small roughness and covering all the surface of the substrate. The results which deduced from optical properties shows that the films have high transmittance with low absorption in the visible region. The optical energy gap values were (3.75, 3.8 and 3.85 eV) of films prepared at (250, 300, 350 ℃) respectivly. The electrical results shows that junctions are abrupt type and values of built in voltage of the prepared junctions 250, 300, 350 ℃ were 1.1, 0.7 and 0.5 respectively.

1. Introduction

Semiconductor nanomaterials possess unique physical and chemical properties that make them suitable for application in emerging technologies, such as, energy conversion, detection devices, miniature sensors, biomedicine, nanoscale imaging, solar cells, nanoelectronics [1,2]. Most transparent conductive oxide (TCO) are based on In_2O_3, SnO_2, ZnO and their mixed compounds. Among them Zinc oxide (ZnO) have excellent attention due to wide optical band gap (Eg=3.37 eV), high transmittance in the visible region, chemical stability, good electron mobility, low resistivity, etc. [3-5]. These features make it to be used in many optoelectronic applications such as laser diode [6,7], sensor [8], solar cell [9, 10] and so on. Various methods have been used to preparation ZnO in thin film form. These includes physical and chemical techniques such as; sputtering [11,12], sol-gel technique [13], pulsed laser deposition (PLD) [14,15], spray pyrolysis [16], physical vapour deposition (PVD) [17], This work deals with preparation and characterization of nanocrystalline ZnO thin film deposited on p- type pours Silicon.

2. Experimental details

The nanocrystalline ZnO film was deposited on a glass substrate, and the substrate was ultrasonically cleaned with acetone, methanol and distilled water, respectively. The deposition solution was prepared by using 50 ml of zinc chloride ($ZnCl_2$ at a concentration of 0.05 M). The precursor solution was sprayed on the heated glass substrate. The deposition parameters of CSPT are fixed as follows: nozzle-substrate height is 30 cm, spraying time is 4 seconds, and stop time is 20 seconds. The deposition temperatures are (250, 300, and 350) respectively. A silicon wafer (p-type) with a size of 2 cm^2 and a resistivity range of (1.5-4 Ω-cm) and (100) face orientation is immersed in diluted (10 %) hydrofluoric acid (HF) for 10 minutes to remove the native oxide layer. Before the anodization process, in order to ensure as uniform current distribution as

---

*Corresponding author: esp.jamalf.mohamad@uoanbar.edu.iq

possible, a vacuum evaporation system (Balzer BAE 370) was used to coat a 400 nm aluminum layer on the back silicon layer under a vacuum of 10^{-5} mbar. The used etching solvent were: HF acid (47%), high purity ethanol (C_2H_5OH) (99%) and de-ionized water (HF: C_2H_5OH: H_2O =1:1:1 volume ratio). The current density was fixed at 40 mA/cm^2 for 10 minutes. Two schematic diagrams of spray pyrolysis and electrochemical etching technology are shown in Fig. 1.
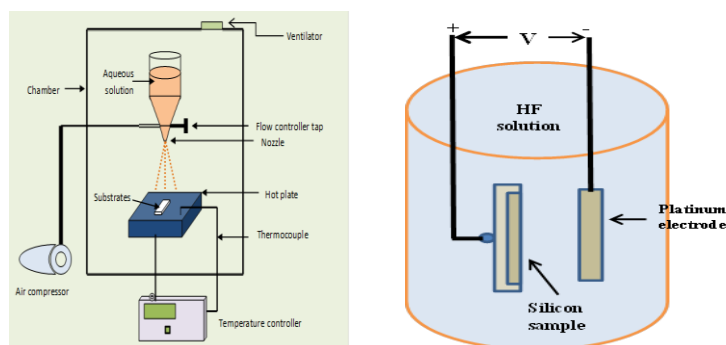

Fig. 1. Schematic diagram of spray pyrolysis (left)[18], and the electrochemical etching (right) techniques.

3. Results and discussion

3.1. Optical properties

Fig. 2 is illustrated transmittance of ZnO thin films deposited on glass substrates at different temperatures (250, 300, 350 ºC) in the range (300-1100 nm). These films have high transmittance in the visible light region. It can be seen that the transmittance increases with increasing temperature. The increase in deposition temperature causes an increase in the evaporation of the solution droplets before reaching the substrate, which leads to a decrease in the film thickness. At the edge of the band, the ZnO film showed a sharp drop, which indicates that the prepared film has good crystallinity. The absorption coefficient (α) is a key role in determining the performance of solar cells. The relationship between absorbance (A) and absorption coefficient is expressed by the following equation:

$$\alpha = \frac{2.3026\ A}{t} \tag{1}$$

Fig. 3 shows the absorption coefficient spectra of ZnO films at three different deposition temperatures in the range (300-1100 nm). The absorption coefficient decreases as the deposition temperature increases and shifts to shorter wavelengths (blue shift). The optical energy band gap (Eg) is related to the absorption coefficient, and the formula is as follows:

$$\alpha h\nu = A\ (h\nu - E_g)^n \tag{2}$$

where; hν- photon energy, n is equal to 2 for allowed direct transition. The variation of the deposited substrate temperature on the optical band gap of the ZnO film is shown in Figure (4). The energy gap increases with the increase of the deposition temperature. The energy gaps at the deposition temperature of 250, 300 and 350ºC are 3.75, 3.8 and 3.85 eV, respectively. These values are larger than the energy gap of bulk ZnO, confirming that these films are nanostructured, which is the result of the quantum confinement effect.
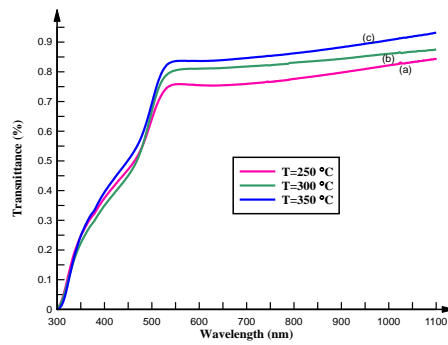
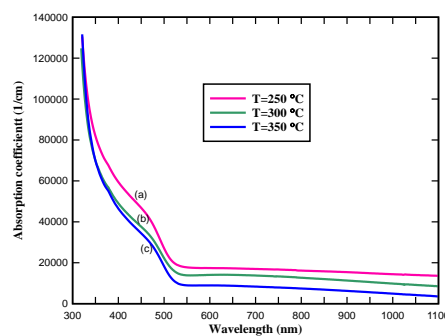*Fig. 2. Transmittance versus wavelength of nanocrystalline ZnO thin film: (a)- T= 250, (b)- T= 300, (c)- T= 350 ºC.*

Fig. 3. Absorption coefficient (α) versus wavelength of nanocrystalline ZnO thin film: (a)- T= 250, (b)- T= 300, (c)- T= 350 ºC.
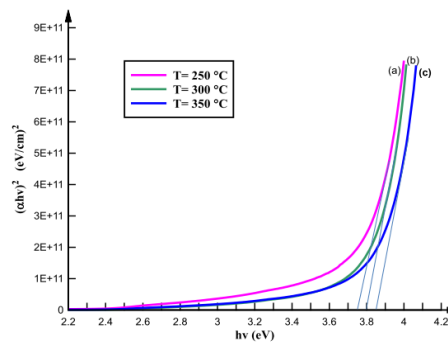

Fig. 4. Energy gap(E_g) versus photon energy (hv) of nanocrystalline ZnO thin film: (a)- T= 250, (b)- T= 300, (c)- T= 350 ºC.

3.2. AFM Analysis

Fig. 5 shows the two-dimensional (2D) and three-dimensional (3D) AFM images of ZnO films. Atomic force microscopy results show that the films prepared at 250, 300, and 350 ºC have a nanocrystalline structure. The distribution of grains is uniform and covers the entire surface. The results also show that the surface roughness decreases as the deposition temperature increases. The decrease in surface morphology will result in a decrease in the reflection of light incident on the film, and this is an important characteristic when the film is used as a window layer in a solar cell. The results obtained are summarized in Table 1.

Table 1. The result of the AFM image of the prepared samples.

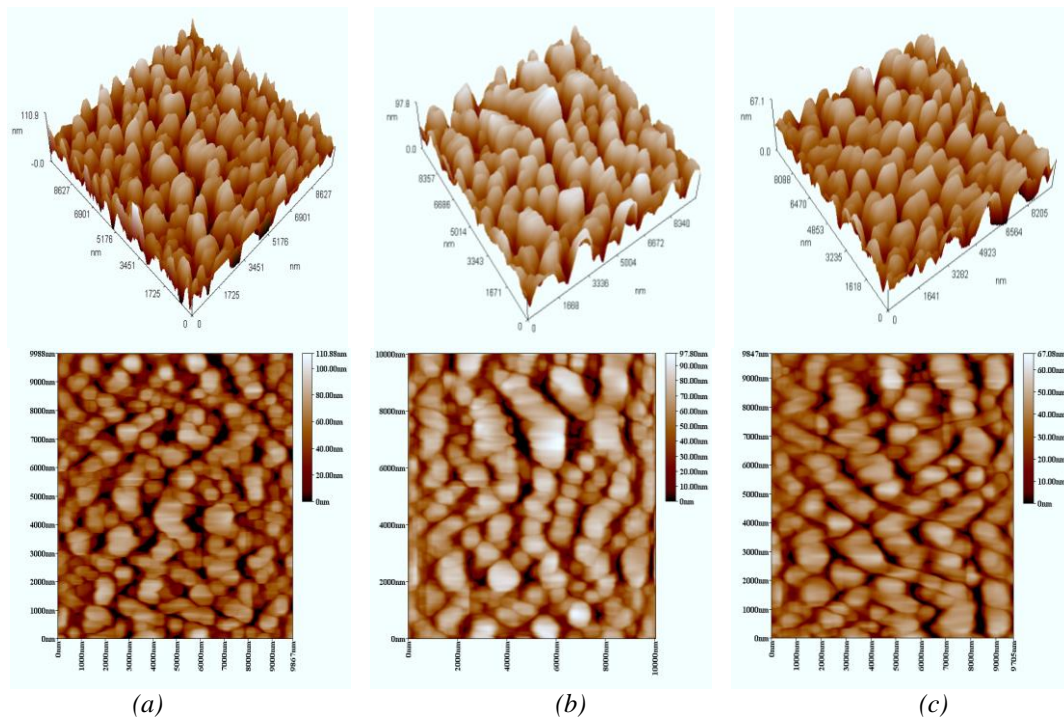| Deposition temperature (ºC)	Root mean square (RMS) (nm)	Roughness average (AR) (nm)	Ten point height (TPH) (nm)	grain size (GS) (nm)
250	22.6	18.8	96	13
300	21.4	17.6	93.6	9
350	13.2	10.7	58.3	6

(a)   *(b)*   *(c)*

Fig. 5. AFM images (2 and 3 2 and 3 dimensions) of nanocrystalline ZnO thin films:
(a)- T= 250, (b)- T= 300, (c)- T= 350 ºC

The electrical characteristics largely depend on the capacitance-voltage characteristics, from which we can obtain many heterojunction parameters, such as: built-in voltage (V_{bi}), junction capacitance and depletion region width. Figure (6) shows the (C-V) characteristics of Al/ZnO/PSi/Al heterojunctions prepared at three different temperatures (250, 300, 350ºC). The results show that for all heterojunctions, the junction capacitance is inversely proportional to the bias voltage. The capacitance decreases as the reverse voltage increases, which increases the built-in potential due to the increase in the width of the depletion layer. Figure (7) shows that C^{-2} as a function of the reverse voltage (V) of the Al/ZnO/PSi/Al heterojunction. Obviously, due to the linear relationship between C^{-2} and the reverse applied voltage, the junction is abrupt, which means a constant depletion layer, so the carrier concentration at the depletion layer is constant. The built-in voltage values of (Al/ZnO/PSi/Al) prepared at (250, 300, 350ºC) are 1.1, 0.7 and 0.5 respectively.
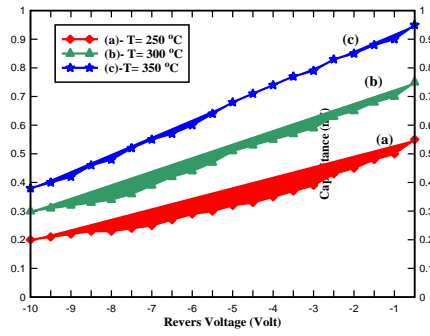
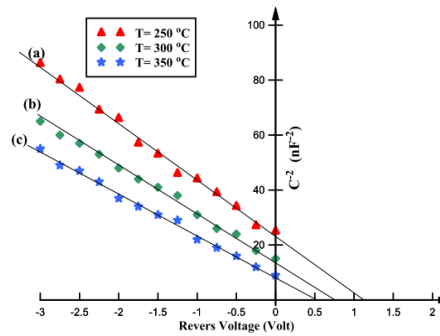*Fig. 6. Capacitance-voltage characteristics of Al/ZnO/PSi/Al, (a)- T= 250, (b)- T= 300, (c)- T= 350 ºC*

Fig. 7. C^{-2} versus applied voltage of Al/ZnO/PSi/Al, (a)- T= 250, (b)- T= 300, c)- T= 350 ºC.

Fig. 8 shows the current-voltage (I-V) characteristics of Al/ZnO/PSi/Al heterojunctions at different temperatures (250, 300, 350ºC). The curves show that devices with these heterojunctions have good rectification behavior. In the case of forward bias, there are two types of current: reombination current and diffusion current of low voltage and high voltage. At low voltages, the width of the depletion layer decreases, so the current increases. At higher voltages, the current-voltage characteristics are almost linear because the depletion layer is minimized at the interface and the porous silicon acts as a series resistance. In all cases, under the reverse bias, at the same voltage value, the reverse current slightly increases with the applied voltage, which causes the generation of electron-hole pairs. At temperatures (250, 300, 350ºC), the ideality factors of Al/ZnO/PSi/Al heterojunctions are 18.7, 13.2 and 6.8, respectively. These values are calculated from the I-V curve using the following equation [19]:

$$n = \frac{q}{k_B T} \frac{\Delta V}{\ln \frac{I}{I_s}}, \tag{1}$$

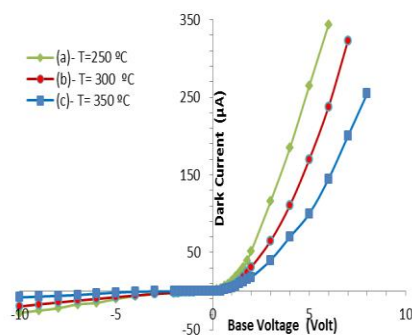where q, I_S and T are the electron charge, saturation current and T is the absolute temperature respectively.

316

Fig. 8. I -V curves of (Al/ZnO/PSi/Al, (a)- T= 250, (b)- T= 300, (c)- T= 350 ºC.

4. Conclusions

The spraying technique was used to successfully deposit nanocrystalline ZnO films on glass and p-type porous silicon at three different temperatures. The prepared film has a high transmittance in the visible light region and and the transmittance increases as the deposition temperature increases. The films prepared at (250, 300, 350ºC) have optical energy gap values (3.75, 3.8 and 3.85 eV) respectively.

The morphological characteristics of the atomic force microscope show that the film has small roughness, uniformity and the crystal grains have a nanocrystalline structure. The above characteristics are the most important requirements for solar cell applications. The electrical properties show that the prepared junction is a abrupt type, and the ideality factors of Al/ZnO/PSi/Al heterojunctions are (18.7, 13.2 and 6.8) at deposition temperatures (250, 300, 350 ºC).

References

[1] S. Suresh, Nanoscience and Nanotechnology **3**, 62 (2013).
[2] G. Murugadoss, J. Mater. Sci. Technol. **28**, 587 (2012).
[3] S. Shariffudin, M. Salina, S. Herman, J. Trans. Electr. Electron. Mater. **13**, 102 (2012).
[4] P. Baviskar, P. Nikam, S. Gargote, A. Ennaoui, B. Sankapal, J. Alloy. Compd. **551**, 233 (2013).
[5] L. M. Wong, S. Y. Chiam, J. Q. Huang, S. J. Wang, W. K. Chim, J. S. Pan, Solar Energy Materials & Solar Cells **95**, 2400 (2011).
[6] K. Kyoungwon, P. C. Debnath, D. H. Lee, Nanoscale, Res. Lett. **6**, 1 (2011).
[7] S. Benramache, F. Chabane, B. Benhaoua, J. Semiconductors **34**, 023001 (2013).
[8] Z. S. Hosseini, A. Irajizad, A. Mortezaali, Sens. Actuators B **207**, 865 (2015).
[9] Morteza Asemi, Morteza Ahmadi, Majid Ghanaatshoar, Ceramics International **44**, 12862 (2018).
[10] S. M. Rozati, Sh. Akesteh, Materials Characterization **58**, 319 (2007).
[11] H. Belaid, M. Nouiri, Z. Ben Ayadi, K. Djessas, L. El Mir, Energy Proceedia **84**, 214 (2015).
[12] Y. M. Tao, S. Y. Ma, H. X. Chen, J. X. Meng, L. L. Hou Y. F. Jia, X. R. Shang, Vacuum **85**, 744 (2011).
[13] U. N. Maiti, P. K. Ghosh, S. Nandy, K. K. Chattopadhyay, Physica B **387**, 103 (2007).
[14] W. Zhaoyang, S. Liyuan, H. Lizhong, Vacuum **85**, 397 (2010).
[15] E. F. Keskenler, G. Turgut, S. Dogan, Superlattices and Microstructures **52**, 107 (2012).
[16] S. Benramache, A. Rahal, B. Benhaoua, Optik **124**, 663 (2013).
[17] Y. S. Kim, W. P. Tai, S. J. Shu, Thin Solid Films **491**, 153 (2005).
[18] J. F. Mohammad, R. I. Mohammed, IOP Conf. Series: Materials Science and Engineering **928**, 072073 (2020).
[19] S. M. Sze, Semiconductor Devices-Physics and technology, 2nd ed.; Wiley: New York, USA, 1985.